

Identical-particle (pion and kaon) femtoscopy in Pb–Pb collisions at $\sqrt{s_{NN}}=5.02$ TeV with Therminator2 modeled with (3+1)D viscous hydrodynamics

Pritam Chakraborty,^{1,*} Ashutosh Kumar Pandey,^{1,2,†} and Sadhana Dash^{1,‡}

¹*Indian Institute of Technology Bombay, Mumbai, India*

²*University of Tsukuba, Japan*

(Dated: October 26, 2020)

The three-dimensional femtosopic correlations of pions and kaons are presented for Pb–Pb collisions at $\sqrt{s_{NN}}=5.02$ TeV within the framework of (3+1)D viscous hydrodynamics combined with THERMINATOR 2 code for statistical hadronization. The femtosopic radii for pions and kaons are obtained as a function of pair transverse momentum and centrality in all three pair directions. The radii showed a decreasing trend with an increase of pair transverse momentum and transverse mass for all centralities. These observations indicate the presence of strong collectivity. A simple effective scaling of radii with pair transverse mass was observed for both pion and kaons.

I. INTRODUCTION

The novel phase of matter characterised by the existence of deconfined state of quarks and gluons is expected to be created at relativistic heavy ion collisions at RHIC and LHC energies [1, 2]. The initial state of the matter is well described by the equations of hydrodynamics and the hydrodynamic collectivity is further ascertained through the measurement of observables like transverse momentum spectra of measured particles, radial and elliptic flow and two-particle angular correlations. However, most of the observables were momentum-based observables and very little was known about the effects of collectivity on spatio-temporal characteristics of particle production and correlation. It is necessary to know the space-time dimension of the system produced in heavy-ion collisions to understand the hydrodynamic collectivity [3, 4]. The extremely small size and lifetime of the system created make it impossible to measure its dimensions directly by any other means. Femtoscopy provides a unique probe to extract the source size of the system by means of studying two particle correlations in momentum space [5]. It incorporates Bose-Einstein (Fermi-Diarc) correlation between two identical particles due to symmetrization (anti-symmetrization) of wave functions of identical bosons (fermions) and Final state interaction (FSI). The analysis is performed in the Longitudinally Comoving System (LCMS), where the pair longitudinal (“long”) axis is along the beam direction, the outward (“out”) axis is along the

transverse momentum of the pair and the “side” axis is perpendicular to the other two axes. In the LCMS, the total momentum of the pairs along the longitudinal direction is conserved. The sizes or the “femtosopic radii” of the system along the *out*, *side* and *long* directions can be expressed as R_{out} , R_{side} and R_{long} , respectively which can be calculated as function of pair transverse momentum and event centrality. The previous measurements at RHIC, BNL at 200 GeV and at LHC, CERN at 2.76 TeV revealed that the system size decreases as the pair transverse momentum (k_T) increases and also, it decreases from central to peripheral events. Besides, at both RHIC and LHC energies, the radii extracted for the pions showed a power-law dependence (scaling) on transverse mass (m_T) and a linear dependence on the final state multiplicity ($\frac{dN_{ch}}{d\eta}$)^{1/3} [6–9]. The findings were consistent with the existence of hydrodynamic collectivity. One expects the scaling of femtosopic radii to be extended to other particle species (such as kaons, protons etc) as they experience the same flow field which the pions were subjected to. A detailed study of the identical particle femtosopic studies using the (3+1)D viscous hydrodynamics coupled with statistical hadronization THERMINATOR 2 model [10, 11] extended the study to kaons and pions and observed an approximate scaling of m_T for pions, kaons and protons in Pb–Pb collisions at $\sqrt{s_{NN}}=2.76$ TeV [12]. However, hadronic re-scattering, resonance decays and other final state interactions can significantly affect the observed scaling. Recent results from PHENIX [13] and ALICE [14] experiments have reported the breaking of the m_T scaling in kaon-kaon correlations while it is not broken for k_T . The hydrokinetic model (HKM) [15, 16] which includes the hydrodynamic phase and a hadronic re-scattering phase

* prchakra@iitb.ac.in

† ashutosh.kumar.pandey@cern.ch

‡ sadhana@phy.iitb.ac.in

described the femtoscopic radii for pions and kaons and predicted the violation of m_T scaling between pion and kaons at LHC energies [17]. The work showed that the approximate scaling was restored when the re-scattering phase was not considered. This indicates the importance of the influence of hadronic re-scattering phase.

In this work, a femtoscopic study of identical pions and kaons have been performed using (3+1D) viscous hydrodynamics coupled with THERMINATOR 2 model at $\sqrt{s_{NN}} = 5.02$ TeV and the m_T and $(\frac{dN_{ch}}{d\eta})^{1/3}$ scaling of the femtoscopic radii have also been reported. The aim of the work is to verify whether the change in freeze-out temperature affects the approximate m_T scaling observed previously at $\sqrt{s_{NN}} = 2.76$ TeV and to provide the initial predictions on the source radii at freeze-out using pion and kaon femtoscopy. Due to the statistical limitations, the femtoscopic calculations for protons have been performed in one dimension together with pions and kaons in the Pair Rest Frame (PRF). The one-dimensional radii for pions, kaons and protons were extracted and the relation between the femtoscopic radii in LCMS and in PRF was explored.

II. INITIAL HYDRODYNAMIC CONDITIONS WITH THERMINATOR 2

THERMINATOR 2 is a Monte Carlo event generator written in C++ with the standard CERN ROOT environment. In this work, the events were generated using the Therminator 2 model which combines the (3 + 1)D viscous hydrodynamics and the statistical hadronisation together with resonance propagation and decay of unstable particles.

The evolution of the flow velocity u^μ and energy density ϵ of the system are solved in (3 + 1)D viscous hydrodynamics model using the second-order Israel-Stewart equations [18]. The energy-momentum tensor, $T^{\mu\nu}$ consists of ideal fluid part, stress tensor $\pi^{\mu\nu}$ and bulk viscosity correction Π [12]. The shear viscosity to entropy density, $\eta/s = 0.08$ was used while bulk viscosity to entropy density, was kept at $\zeta/s = 0.04$. The initial time, τ_i for the hydrodynamic evolution was 0.6 fm/c and the freeze-out temperature is $T_f = 150$ MeV. The chemical potentials were all set to zero.

$$T^{\mu\nu} = (\epsilon + p + \Pi)u^\mu u^\nu + \pi^{\mu\nu} - (p + \Pi)g^{\mu\nu} \quad (1)$$

After hydrodynamic evolution of the system, the event-by-event fluctuations in the initial conditions

produce fluctuating freeze-out hyper-surfaces. The Glauber model was used to obtain the initial density profile in the transverse plane, $\rho_{part} \frac{1-\alpha}{2} + \alpha\rho_{bin}$, where ρ_{bin} and ρ_{part} are the density of binary collisions and participating nucleons, respectively and the mixing parameter, $\alpha = 0.15$ [12]. This analysis has been done for seven sets of impact parameters values (in fm) for Pb-Pb collisions at the $\sqrt{s_{NN}} = 5.02$ TeV. The impact parameters of 2.3, 5.7, 7.4, 8.7, 9.9, 10.9 and 11.9 (in fm), corresponds to the collision events at LHC of different centrality ranges: 0-5%, 10-20%, 20-30%, 30-40%, 40-50%, 50-60% and 60-70%, respectively [12, 28]. The yield of the particles, produced after hadronisation are calculated from the Cooper-Frye formula by THERMINATOR 2 code which uses the freeze-out hypersurfaces obtained from the hydrodynamic calculations as the input [12].

$$E \frac{d^3 N}{dp^3} = \int d\Sigma_\mu p^\mu f(p_\mu u^\mu) \quad (2)$$

where $d\Sigma_\mu$ is the integration element on the freeze-out hypersurface and f is the momentum distribution which includes non-equilibrium corrections to the bulk viscosity (δf_{bulk}) and shear viscosity (δf_{shear}). The details of the modifications of the equilibrium momentum distributions and corrections can be found in [12]:

The THERMINATOR 2 model is based on single freeze-out and there is no difference between the chemical and kinetic freeze-out of the system. This model includes all known resonances in hadronisation along with their propagation and decay. The particles are assumed to be created either on the freeze-out hypersurface or from the subsequent decay of unstable particles.

III. IDENTICAL-PARTICLE FEMTOSCOPY METHODOLOGY

The femtoscopy method relies on two particle correlations originating primarily from wave function (anti)symmetrization commonly known as the Quantum Statistics (QS) effect. In this work, the formalism outlined in reference [12] has been followed to obtain the correlation function. The correlation function is defined as the ratio of probability of observing two particles with different momentum simultaneously to the probabilities of observing each of them separately. It can be constructed by finding the ratio of the relative momentum distribution of particle pairs produced in same event to the distribution of particle pairs se-

lected from different events. The other sources of correlation namely the final state interactions due to Coulomb and Strong interaction between the particle pairs is not included. The effect of QS is incorporated as an afterburner and is considered to be the only source of correlation in this analysis. If Ψ is the pair wave-function, it has to be symmetrized for the identical bosons e.g. pions, kaons and can be expressed as [12]

$$\Psi_{K,\pi} = 1 + \cos(2\mathbf{k}^* \cdot \mathbf{r}^*), \quad (3)$$

and for the identical fermions e.g. protons, it can be expressed as [12]

$$\Psi_p = 1 - \frac{1}{2} \cos(2\mathbf{k}^* \cdot \mathbf{r}^*), \quad (4)$$

Theoretically, one can express the correlation function, $C(\mathbf{k}^*)$ as [12]

$$C(\mathbf{k}^*) = \frac{\int \mathbf{S}(\mathbf{r}^*, \mathbf{k}^*) |\Psi(\mathbf{r}^*, \mathbf{k}^*)|^2}{\int \mathbf{S}(\mathbf{r}^*, \mathbf{k}^*)} \quad (5)$$

where \mathbf{r}^* is the relative space-time separation of two particles at the time of generation, \mathbf{k}^* is half of the pair relative momentum i.e. momentum of the first particle at Pair Rest Frame (PRF) and \mathbf{S} is the source function which corresponds to the probability of the emission of pair of particles. Ψ is the pair wave-function and hence accounts for the mutual interactions between the particles in the pair.

The correlation function has been constructed by filling two histograms, namely **Num** and **Den** for pairs of identical particles for a given centrality class. The charged pions or kaons generated from Therminator 2 events were combined to form pairs. The **Num** histogram was filled with particle pairs corresponding to relative momenta $\mathbf{q} = 2\mathbf{k}^*$ from same events. The pair weight for a particular k_T bin was calculated from Eq.(3) for pions and kaons and from Eq.(4) for protons. The **Den** histogram was filled with pairs where a particle is selected from mixed events and the weight given while filling was 1.0. These histograms can be expressed as a function of three components of \mathbf{q} (three dimensional), $|\mathbf{q}|$ (one dimensional) only, or as a set of one-dimensional histograms corresponding to spherical harmonics representation of the pair distribution. The correlation function was calculated as $C = Num/Den$.

In order to estimate the femtoscopic radii of the system, the source function was assumed to be a three-dimensional ellipsoid with Gaussian density profile [12]:

$$S(\mathbf{r}) \approx \exp\left(-\frac{r_{out}^2}{4R_{out}^2} - \frac{r_{side}^2}{4R_{side}^2} - \frac{r_{long}^2}{4R_{long}^2}\right) \quad (6)$$

where r_{out} , r_{side} and r_{long} were the components of \mathbf{r}^* calculated in LCMS and R_{out} , R_{side} and R_{long} correspond to single-particle femtoscopic source radii, in transverse, side and longitudinal directions, respectively.

The radii in different directions were extracted by fitting the following function to the correlation function [12] obtained from Eq.(5):

$$C(\mathbf{q}) = 1 + \lambda \exp(-R_{out}^2 q_{out}^2 - R_{side}^2 q_{side}^2 - R_{long}^2 q_{long}^2), \quad (7)$$

where, λ accounts for the strength of the correlation which signifies that not all pairs considered were correlated and the assumed functional form of the source was not exactly Gaussian Eq.(5).

Similarly, the functional form of the source for one-dimensional correlation function was assumed to be spherically symmetric in PRF and can be expressed as [12]:

$$S(\mathbf{r}^*) \approx \exp\left(-\frac{\mathbf{r}^{*2}}{4R_{inv}^2}\right), \quad (8)$$

where R_{inv} is the source size.

The one-dimensional fitting function was [12]:

$$C(q_{inv}) = 1 + \lambda \exp(-R_{inv}^2 q_{inv}^2). \quad (9)$$

The transformation from LCMS to PRF was performed by a Lorentz boost along the pair transverse momentum with velocity $\beta_T = \frac{p_T}{m_T}$. This also indicates that in the PRF, the R_{side} and R_{long} remain unchanged and only the R_{out} changes according to the Eq. 10.

$$R_{out}^* = \gamma_T R_{out} \quad (10)$$

where, the “*” corresponds to the quantity in PRF and $\gamma_T = \frac{1}{\sqrt{1-\beta_T^2}}$ is the Lorentz factor of the transverse boost.

IV. RESULTS AND DISCUSSION

The correlation functions of pion and kaons were obtained for six centrality classes. For each centrality class, the correlation functions were obtained in the k_T ranges of (0.1-0.2), (0.2-0.3), (0.3-0.4), (0.4-0.5), (0.5-0.6), (0.6-0.7) and (0.7-0.8) (in GeV/c) for pion-pion pairs while for kaon pairs, the k_T ranges started from 0.3 GeV/c due to low statistics of kaon pairs in low k_T bins.

In Figure 1, the radii for pions in LCMS are shown as a function of k_T for different centrality classes in three directions, transverse (*out*), side and longitudinal (*long*). The radii in all directions decrease with an increase in k_T for different centrality classes. The maximum values of radii in both the transverse and side direction, R_{out} and R_{side} are observed to be of the order of 7 fm for the lowest k_T bin for most central (0-5%) collisions. The maximum value of the radius along the longitudinal direction, R_{long} in most central collisions is of the order of 11 fm for the lowest k_T range. The lowest radii in all three directions are found to be ~ 2 fm, for highest k_T range and for 50-60% centrality.

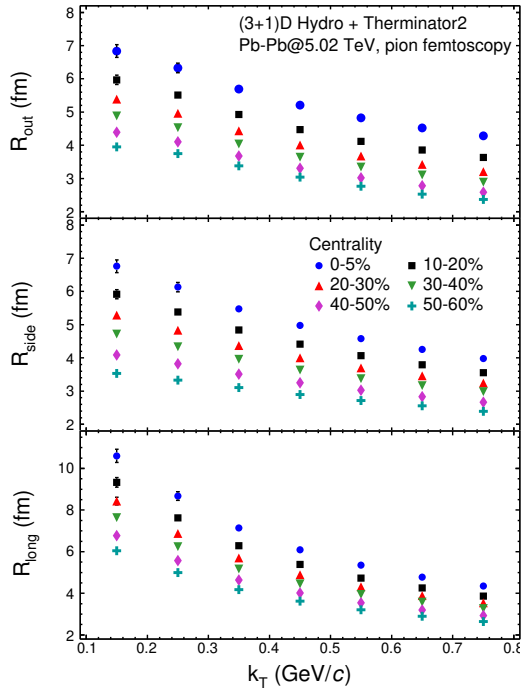


FIG. 1. (Color online) The femtoscopic radii for pions in LCMS as a function of pair transverse momentum for different centralities for Pb–Pb collisions at $\sqrt{s_{NN}} = 5.02$ TeV using Therminator 2 model.

Direction	Centrality (%)	A	B
<i>out</i>	0-5	3.88 ± 0.04	-0.38 ± 0.02
	30-40	2.61 ± 0.02	-0.42 ± 0.01
	50-60	2.17 ± 0.02	-0.42 ± 0.01
<i>side</i>	0-5	3.58 ± 0.04	-0.42 ± 0.02
	30-40	2.73 ± 0.02	-0.30 ± 0.01
	50-60	2.26 ± 0.02	-0.30 ± 0.01
<i>long</i>	0-5	3.61 ± 0.04	-0.69 ± 0.01
	30-40	2.74 ± 0.02	-0.65 ± 0.01
	50-60	2.24 ± 0.02	-0.63 ± 0.01

TABLE I. The parameters obtained from the power-law fit of the radii along *out*, *side* and *long* direction as a function of m_T for pion-femtoscopy for selected centralities for Pb–Pb collisions at $\sqrt{s_{NN}} = 5.02$ TeV using Therminator 2 model

In Figure 2, the radii for pions in LCMS are shown as a function of transverse mass, m_T for different centralities. The radii decrease as a function of m_T for all centralities. The dashed lines shown for few centralities are power-law fits to the radii and it can be seen that the variation of radii with m_T is well described by the power-law function. The functional form of the power law used is given by[12]:

$$f(m_T) = A \times m_T^B, \quad (11)$$

where A and B are the free parameters. The values of the extracted fits are shown in Table I. As can be seen from the table, for *out* direction, and *side* direction, B is of similar value for all centrality classes while it is higher for the *long* direction,

In Fig. 3, the dependence of radii of pions on the final-state multiplicity for different k_T ranges has been shown. It is observed that the radii in all directions decrease from most central events to peripheral events. The values are fitted with a linear function given by:

$$f\left(\left\langle \frac{dN_{ch}}{d\eta} \right\rangle^{\frac{1}{3}}\right) = C + D \times \left\langle \frac{dN_{ch}}{d\eta} \right\rangle^{\frac{1}{3}}, \quad (12)$$

for some selected k_T ranges. The values of the extracted parameters are shown in Table II. In all three directions, D decreases for higher k_T regions.

The scaling of m_T and $(\frac{dN_{ch}}{d\eta})^{1/3}$ shows the presence of collective flow in both the transverse dimensions [12].

The variation of radii for kaons in LCMS as a

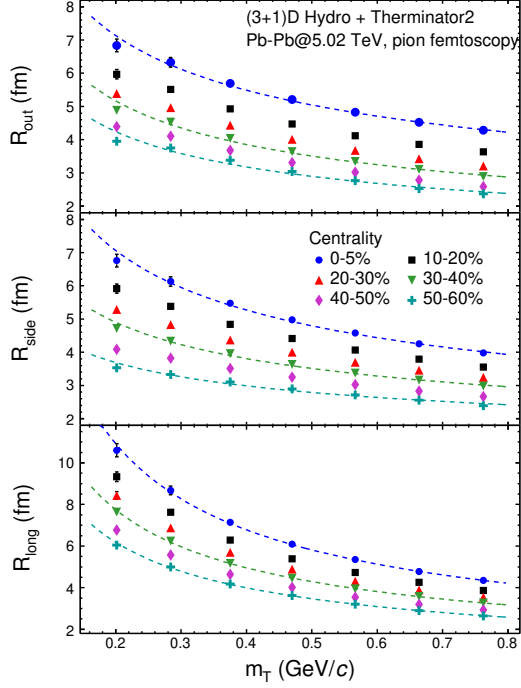


FIG. 2. (Color online) The femtosopic radii for pions in LCMS as a function of pair transverse mass at different centralities for Pb–Pb collisions at $\sqrt{s_{NN}} = 5.02$ TeV using Thermanator 2 model.

Direction	k_T (GeV/c)	C	D
<i>out</i>	0.1-0.2	1.44 ± 0.15	0.42 ± 0.02
	0.4-0.5	1.20 ± 0.07	0.30 ± 0.01
	0.6-0.7	0.81 ± 0.05	0.28 ± 0.01
<i>side</i>	0.1-0.2	0.61 ± 0.14	0.49 ± 0.02
	0.4-0.5	1.04 ± 0.07	0.31 ± 0.01
	0.6-0.7	1.04 ± 0.05	0.25 ± 0.01
<i>long</i>	0.1-0.2	1.99 ± 0.25	0.68 ± 0.03
	0.4-0.5	1.45 ± 0.09	0.36 ± 0.01
	0.6-0.7	1.22 ± 0.06	0.28 ± 0.01

TABLE II. The parameters obtained from the linear fit of the radii along *out*, *side* and *long* direction as a function of $\langle dN_{ch}/d\eta \rangle^{\frac{1}{3}}$ for pion-femtoscopy for selected centralities for Pb–Pb collisions at $\sqrt{s_{NN}} = 5.02$ TeV using Thermanator 2 model

function of k_T and m_T for different centralities are shown in Fig. 4 and Fig. 5, respectively. The radii decrease with k_T and m_T for the considered centrality classes and also from most central to peripheral events. The trend is similar to the one observed for pions. The dashed lines in Figure 5

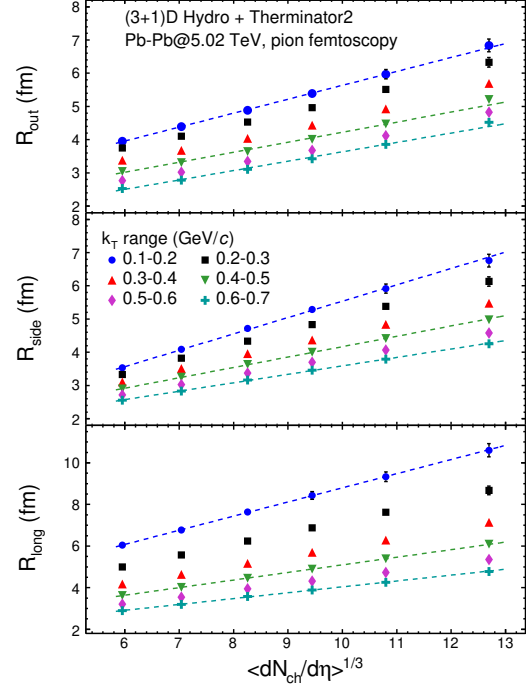


FIG. 3. (Color online) The femtosopic radii of pions as a function $\langle \frac{dN_{ch}}{d\eta} \rangle^{\frac{1}{3}}$ for several k_T ranges for Pb–Pb collisions at $\sqrt{s_{NN}} = 5.02$ TeV using Thermanator 2 model

depict the power law fits (given by Eq. 11.) to the radii values. The extracted fit parameters are shown in Table III. Figure 6, shows the final-state multiplicity dependence of the radii for kaons in different k_T ranges. The radii increases monotonically from peripheral to central events for different k_T ranges in all three directions. The statistical uncertainties in the radii at lower multiplicity region is relatively larger in all directions. The values have been fitted with Eq. 12 for some selected k_T ranges and the values are shown in Table IV.

One can observe that the slopes of m_T dependence of kaon radii are quite different from the pions. To test the hypothesis of common effective scaling for m_T , the pion and kaon radii have been plotted simultaneously as a function of m_T for some selected centralities and they have been fitted with the power-law function of m_T given by Eq. 11. The fit parameters are that of pions. It can be seen from the figure that the m_T scaling is approximately followed in *out* and *side* direction while it is slightly violated for (0-20)% and (20-30)% centrality in *long* direction. From these observations, it is clear that the (3+1)D Hydro + THERMI-

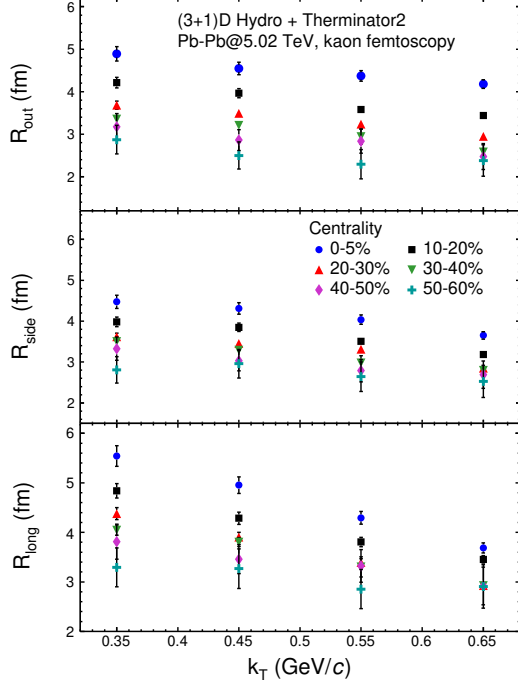


FIG. 4. (Color online) The femtosopic radii for kaons in LCMS as a function of m_T for different centralities for Pb–Pb collisions at $\sqrt{s_{NN}} = 5.02$ TeV using Thermanator model 2.

NATOR 2 model predicts an approximate scaling of the three-dimensional femtosopic radii as function of pair m_T in LCMS for pions and kaons which has also been claimed in the femtosopic study of identical particles produced in Pb–Pb collision at $\sqrt{s_{NN}} = 2.76$ TeV modeled in (3+1)D hydrodynamics [12]. The femtosopic radii for protons in LCMS could not be included in this observation due to the statistical limitations but from this scaling, we can predict the radii of not only protons but heavier particles also. Both R_{out} and R_{side} radii are influenced by flow and re-scatterings, and thus their ratio becomes a robust observable which is not affected by these effects. Figure 8 also shows the m_T dependence of the ratio R_{out}/R_{side} for pions and kaons. It can be seen that the values for kaons are slightly lower than that of pions for (0-5)% centrality while it is mildly higher than pions for peripheral collisions. However, the statistical uncertainties are large and one cannot make any conclusions about the different space-time correlations for these two particle species.

The extraction of femtosopic radii in three dimensions and in different centrality classes for heavier particles like kaons and protons are some-

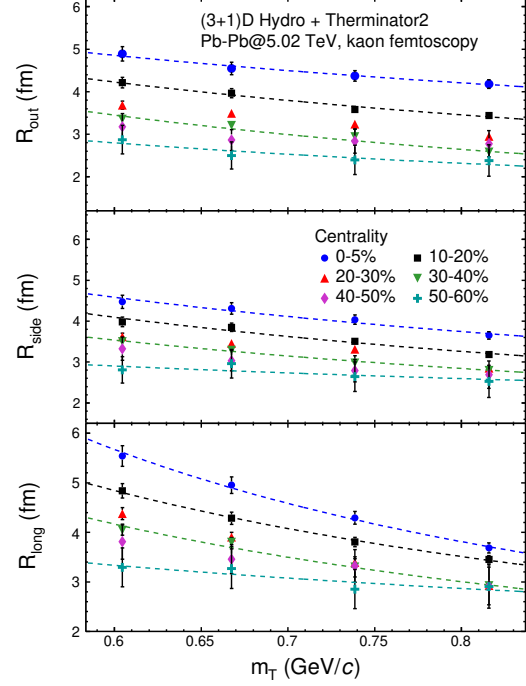


FIG. 5. (Color online) The femtosopic radii for kaons in LCMS as a function of pair transverse mass at different centralities for Pb–Pb collisions at $\sqrt{s_{NN}} = 5.02$ TeV using Thermanator 2 model.

times limited by statistics. Therefore, a measurement of one-dimensional radius in the PRF (pair rest frame) is often performed. The R_{inv} is a direction-averaged source size in PRF and can be obtained by fitting the one-dimensional correlation function with Eq. 9 in PRF [12] which assumes that the source is Gaussian. The system in LCMS can be Lorentz boosted in the direction of pair transverse momentum to PRF to obtain the radii R_{out}^* , R_{side}^* and R_{long}^* in the PRF. An effective radius, R_{eff} , can be calculated by taking the mean of R_{out}^* , R_{side}^* and R_{long}^* and can be compared to R_{inv} . In Fig. 9, the R_{inv} for pions and kaons (obtained from a fit of Eq. 9 to the one-dimensional correlation function) have been compared with the R_{eff} calculated from the corresponding R_{out} , R_{side} and R_{long} obtained by fitting three dimensional correlation function in LCMS and also the corresponding γ_T . One can observe that there is a good agreement between the R_{inv} and the corresponding R_{eff} and the differences are within 7%. This indicates that once can determine R_{inv} from the values of R_{out} , R_{side} and R_{long} obtained in LCMS and from the Lorentz boost factor.

Due to statistical limitations of performing

Direction	Centrality (%)	A	B
<i>out</i>	0-5	3.77 ± 0.17	-0.50 ± 0.13
	10-20	2.96 ± 0.11	-0.70 ± 0.11
	30-40	2.15 ± 0.07	-0.75 ± 0.09
	50-60	2.00 ± 0.50	-0.65 ± 0.63
<i>side</i>	0-5	3.20 ± 0.15	-0.70 ± 0.13
	10-20	2.73 ± 0.10	-0.79 ± 0.11
	30-40	2.40 ± 0.08	-0.76 ± 0.09
<i>long</i>	0-5	2.80 ± 0.14	-1.38 ± 0.14
	10-20	2.74 ± 0.11	-1.11 ± 0.12
	30-40	2.33 ± 0.07	-1.13 ± 0.09
	50-60	2.55 ± 0.60	-0.52 ± 0.60

TABLE III. The parameters obtained from the power-law fit of the radii along *out*, *side* and *long* direction as a function of m_T for kaon-femtoscopy for selected centralities for Pb–Pb collisions at $\sqrt{s_{NN}} = 5.02$ TeV using Therminator 2 model

Direction	k_T (GeV/c)	C	D
<i>out</i>	0.3-0.4	0.69 ± 0.32	0.32 ± 0.03
	0.4-0.5	0.72 ± 0.28	0.30 ± 0.03
	0.5-0.6	0.21 ± 0.33	0.32 ± 0.03
	0.6-0.7	0.30 ± 0.20	0.29 ± 0.02
<i>side</i>	0.3-0.4	1.66 ± 0.32	0.22 ± 0.03
	0.4-0.5	1.43 ± 0.28	0.22 ± 0.03
	0.5-0.6	0.59 ± 0.32	0.27 ± 0.03
	0.6-0.7	1.25 ± 0.20	0.18 ± 0.02
<i>long</i>	0.3-0.4	1.37 ± 0.39	0.32 ± 0.04
	0.4-0.5	1.75 ± 0.33	0.24 ± 0.04
	0.5-0.6	1.28 ± 0.36	0.23 ± 0.03
	0.6-0.7	1.40 ± 0.21	0.18 ± 0.02

TABLE IV. The parameters obtained from the linear fit of the radii along *out*, *side* and *long* direction as a function of $\langle dN_{ch}/d\eta \rangle^{1/3}$ for kaon pairs for selected centralities for Pb–Pb collisions at $\sqrt{s_{NN}} = 5.02$ TeV using Therminator 2 model

the 3-D femtosopic studies of proton, the one-dimensional radius R_{inv} in PRF for protons was obtained with this model. As a common effective m_T scaling have been observed for radii of pion and kaon in LCMS and R_{inv} was shown to be directly related to them, one expects to observe a similar scaling of R_{inv} for pions, kaons and protons also. However, for the same m_T , γ_T would be different for pions and kaons and the difference would be

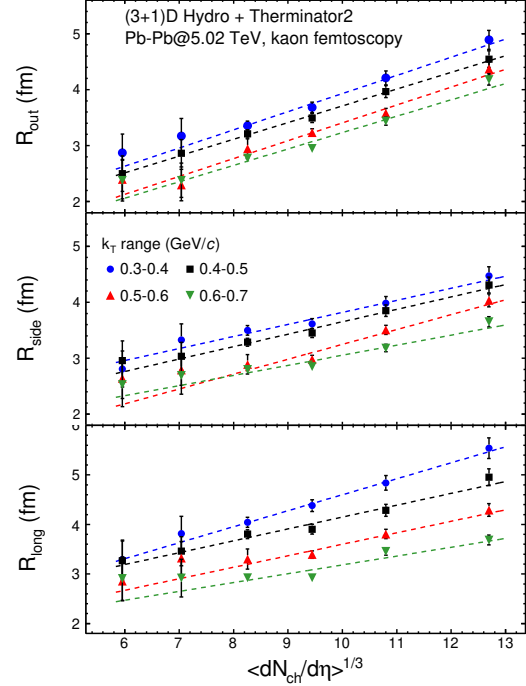


FIG. 6. (Color online) The femtosopic radii for kaons as a function of cube root of the charged particle multiplicity for several k_T ranges for Pb–Pb collisions at $\sqrt{s_{NN}} = 5.02$ TeV using Therminator 2 model

more for protons also. This would result in different R_{out}^* values for pions, kaons and protons for the same m_T bin. Therefore R_{inv} of pions, kaons and protons are expected to differ for same m_T . Fig. 10 shows the R_{inv} for pions, kaons and protons in PRF as a function of m_T for different centralities classes. It can be clearly seen in the upper panel of the figure that pions, kaons and protons show different trends for different centralities at similar m_T .

As discussed previously, the violation of scaling in R_{inv} can be attributed to difference in Lorentz boost factors for different particles. The one dimensional radii therefore can be scaled by the following factor

$$f = (\gamma_T + 2)/3, \quad (13)$$

It can be seen that a common scaling for pions, kaons and protons is observed and is seen in lower panel of Fig. 10. The form of this scaling factor is described in [12]. Thus, the measurement of the one-dimensional radius of different particle species in PRF can give important information for search of collectivity scaling in experimental data analysis.

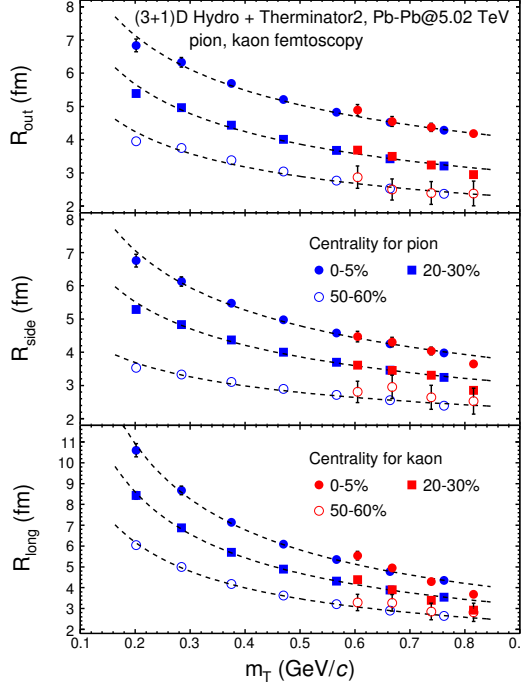


FIG. 7. (Color online) The femtosopic radii in LCMS for pions and kaons for selected centralities for Pb–Pb collisions at $\sqrt{s_{NN}} = 5.02$ TeV using Thermanator 2 model. Lines represent power-law fits to the combined pion and kaon data points at a given centrality and direction.

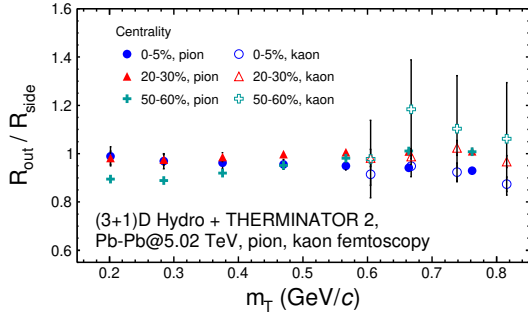


FIG. 8. (Color online) R_{out}/R_{side} as a function of m_T for pions and kaons for different centrality classes for Pb–Pb collisions at $\sqrt{s_{NN}} = 5.02$ TeV using Thermanator 2 model.

V. CONCLUSION

The femtosopic radii extracted from system of identical pions, kaons and protons using (3+1)D hydrodynamic model coupled with THERMINATOR 2 code for statistical hadronization, resonance propagation and decay has been studied as

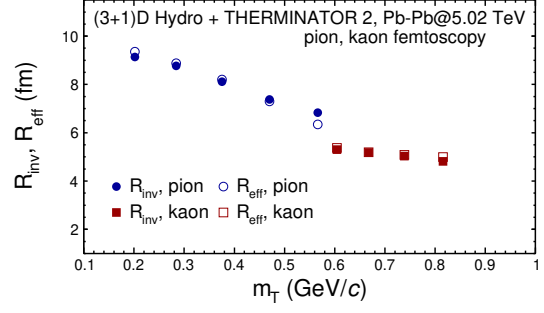


FIG. 9. (Color online) Comparison of the R_{inv} obtained directly from the fit to the one-dimensional correlation function in PRF and a result R_{eff} of the approximate procedure to estimate R_{inv} from values of R_{out} , R_{side} and R_{long} measured in LCMS

a function of centrality and pair transverse mass, m_T . The effect of hadronic re-scattering has not been considered in this model. The obtained radii decreased from central to peripheral collisions as well as with an increase of m_T . In the LCMS frame, the radii followed two mutually exclusive effective scaling, a power law scaling with pair m_T and a linear scaling with $\langle dN_{ch}/d\eta \rangle^{\frac{1}{3}}$. The slope for $\langle dN_{ch}/d\eta \rangle^{\frac{1}{3}}$ scaling was observed to be almost similar in all the three directions (*out*, *side* and *long*). For the m_T scaling, the curves in *out* and *side* directions were less steeper compared to *long* direction which corresponds to the larger flow velocity [22]. A violation of such scaling was observed recently in LHC data for kaons and in other hydrodynamical models which incorporated the effects of hadronic re-scattering. Therefore, violation of such scalings in experimental data probes the relevance of hadronic re-scattering phase. The one-dimensional femtosopic radii R_{inv} in PRF have also been studied as a function of centrality and pair m_T . A power-law m_T scaling, similar to the three dimensional radii measured in LCMS, have also been observed for R_{inv} though the scalings in LCMS and PRF were independent to each other. A common effective scaling of R_{inv} for pions, kaons and protons was observed after scaling the obtained R_{inv} with a kinematic factor arising due to difference in Lorentz factors for different species of particles.

VI. ACKNOWLEDGEMENTS

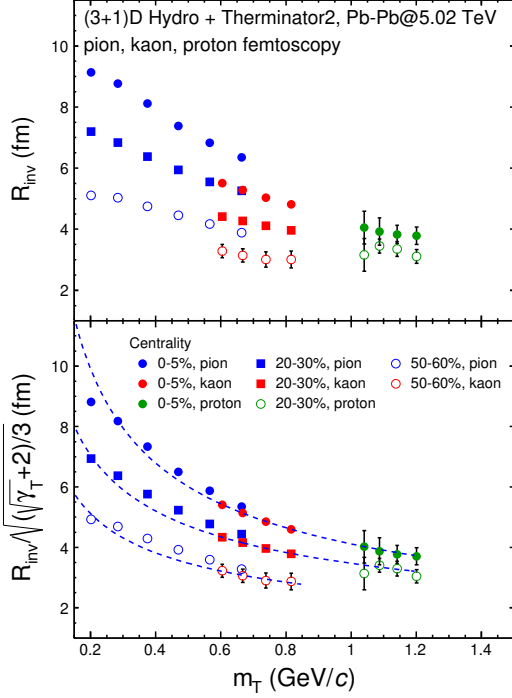


FIG. 10. (Color online) a) One-dimensional femtoscopic radius R_{inv} for pions, kaons and protons calculated in the PRF for selected centralities. (b) R_{inv} for pions, kaons and protons scaled with the kinematic factor, for selected centralities (see text for details). Lines represent power-law fits

The authors would like to thank Department of Science and Technology (DST), Government of India for supporting the present work. The authors would also like to thank Piotr Bozek for providing the files with hypersurfaces from the (3+1) dimensional perfect hydrodynamics.

-
- [1] J. Adams *et al.* (STAR Collaboration), Nucl. Phys. **A 757**, 102-183 (2005).
[2] K. Adcox *et al.* (STAR Collaboration), Nucl. Phys. **A 757**, 184-283 (2005).
[3] Yu. M. Sinyukov, S. V. Akkelin, I. A. Karpenko, and Y. Hama, Acta Phys. Polon. **B40**, 1025-1036 (2009).
[4] W. Broniowski, M. Chojnacki, W. Florkowski, and A. Kisiel, Phys. Rev. Lett. **101**, 022301, (2008)
[5] M. A. Lisa, S. Pratt, R. Soltz, and U. Wiedemann, Ann. Rev. Nucl. Part. Sci. **55**, 357–402, (2005)
[6] J. Adams *et al.* (STAR Collaboration), Phys. Rev. C **71**, 044906 (2005).
[7] B. I. Abelev *et al.* (STAR Collaboration), Phys. Rev. C **80**, 024905 (2009).
[8] S. Afanasev *et al.* (PHENIX Collaboration), Phys. Rev. Lett. **103**, 142301 (2009)
[9] K. Aamodt *et al.* (ALICE Collaboration), Phys. Lett. **B696**, 328 (2011).
[10] A. Kisiel, T. Taluc, W. Broniowski and W. Florkowski, Comput. Phys. Commun. **174**, 669 (2006) doi:10.1016/j.cpc.2005.11.010 [nucl-th/0504047].
[11] M. Chojnacki, A. Kisiel, W. Florkowski and W. Broniowski, Comput. Phys. Commun. **183**, 746 (2012) doi:10.1016/j.cpc.2011.11.018 [arXiv:1102.0273 [nucl-th]].
[12] A. Kisiel, M. Gałazyn, and P. Bożek, Phys. Rev. C **90**, 064914 (2014)
[13] A. Adare *et al.* (PHENIX Collaboration), Phys. Rev. C **92** no. 3, 034914 (2015)
[14] S. Acharya *et al.* (ALICE Collaboration), Phys. Rev. C **96**, 064613 (2017)
[15] I. A. Karpenko, Yu. M. Sinyukov, and K. Werner, Phys. Rev. C **87**, 024914 (2013)
[16] I. A. Karpenko and Yu. M. Sinyukov, Phys. Rev. C **81**, 054903 (2010)
[17] V. M. Shapoval, P. Braun-Munzinger, I. A. Karpenko, and Yu.M. Sinyukov, Nucl. Phys. **A 929**,1 (2014)
[18] C. Gale, S. Jeon, B. Schenke, P. Tribedy, and R. Venugopalan, Phys. Rev. Lett. **110**, 012302 (2013).
[19] P. Bozek, Phys. Rev. C **85**, 034901 (2012)

- [20] A. Kisiel and D. A. Brown, Phys. Rev. C **80**, 064911 (2009).
- [21] S. V. Akkelin and Y. M. Sinyukov, Phys. Lett. B **356**, 525 (1995).
- [22] B. Tomasik and U. W. Heinz, Eur. Phys. J. C **4**, 327 (1998).
- [23] W. Broniowski, M. Chojnacki, W. Florkowski, and A. Kisiel, Phys. Rev. Lett. **101**, 022301 (2008).
- [24] S. Pratt, Nucl. Phys. A **830**, 51C (2009).
- [25] S. Borsanyi *et al.*, J. High Energy Phys. **11** (2010) 077.
- [26] P. Bozek, Phys. Rev. C **89**, 044904 (2014).
- [27] P. Bozek and I. Wyskiel-Piekarska, Phys. Rev. C **85**, 064915 (2012).
- [28] K. Aamodt *et al.* (ALICE Collaboration), Phys. Rev. Lett. **106**, 032301 (2011).